Review

Emerging Luminescent Materials for Information Encryption and Anti-Counterfeiting: Stimulus-Response AIEgens and Room-Temperature Phosphorescent Materials

Yanjie Li [1] and Pengfei Gao [1,2,*]

[1] Key Laboratory of Luminescence Analysis and Molecular Sensing (Southwest University), Ministry of Education, College of Pharmaceutical Sciences, Southwest University, Chongqing 400715, China; lyj1989@swu.edu.cn

[2] NMPA Key Laboratory for Quality Monitoring of Narcotic Drugs and Psychotropic Substance, Chongqing 401121, China

[*] Correspondence: shandonggaopengfei@163.com

Abstract: Information encryption and anti-counterfeiting play an important role in many aspects of daily life, such as in minimizing economic losses, protecting secure communication and public security, and so on. Owing to the high information capacity and ease of operation, luminescent materials for advanced information encryption and anti-counterfeiting are essential to meet the increasing demand on encryption security. Herein, we summarize two emerging luminescent materials for information encryption and anti-counterfeiting—AIE materials and room-temperature phosphorescent materials. Finally, we discuss the opportunities and anticipations of these two information encryption and anti-counterfeiting materials.

Keywords: AIEgens; RTP materials; information encryption; anti-counterfeiting; multilevel encryption

1. Introduction

With the rapid development of economy, the amount of fake products and information is rapidly increasing [1,2]. In such case, information encryption and anti-counterfeiting technologies are essential to minimize economic losses and protect public security [3], and have always been considered a major challenge. Up to now, there have been various designs for information encryption and anti-counterfeiting, which are based on different stimuli-responsive materials, such as the thermochromic photonic crystal [4], photore-sponsive liquid crystal lasing materials [5], time-dependent luminescent materials [6,7], anisotropically shaped complex materials [8], circularly polarized luminescence (CPL) materials [9–11], and so on. In addition, numerous functional materials with multimodal emission have also been investigated and used for advanced information encryption and anti-counterfeiting [12]. Attributed to the single particle analysis accuracy of dark-field microscopy (DFM) imaging [13–17], the single particle level data encryption could also be achieved recently [18].

Among these intelligent response materials, luminescent materials are most widely used, which can always be easily regulated by various external stimuli such as chemical reagents, heat, mechanical force, excitation light, and acidity or alkalinity. The output signals are abundant and can range from elementary parameters, such as emission intensity and emission color, to dynamic parameters, such as emission duration time and the discoloration process. Furthermore, the incident light has rich dimensions (wavelength, excitation duration, polarization, and power), and thus the multilevel stimulus can effectively improve the security level [19,20].

Most of the luminescent materials used for information encryption and anti-counterfeiting are used in the form of aggregated and solid state. So, the aggregated materials should display

excellent luminescent properties. As known, the aggregates always show completely different properties and behaviors to the dispersed molecules [21,22]. The aggregation-induced emission (AIE) phenomenon meets this requirement that the luminescence in the aggregated state is much better. AIE materials contain not only the commonly used aggregation-induced emission luminogens (AIEgens), but also materials that exhibit properties like CPL, aggregation-induced delayed fluorescence (AIDF), room-temperature phosphorescence (RTP), clusterization-triggered emission (CTE), and so on [23]. In this review, part of AIEgens- and RTP-materials-based designs and applications for information encryption and anti-counterfeiting are introduced.

We hope this review will offer insight into AIEgens- and RTP-materials-based technologies and their recent applications in information encryption and anti-counterfeiting to help further develop and update this technique.

2. Application of AIE Materials in Information Encryption and Anti-Counterfeiting

The concept of AIE was first proposed in 2001 [24] and is a phenomenon different from traditional aggregation-caused quenching (ACQ). After two decades, AIE has developed into a thriving field, and AIEgens have been widely investigated and applied in various fields [25], such as theranostics [26–28], biosensing [29–31], organic luminescent materials [32,33], and metal batteries [34]. For information encryption and anti-counterfeiting applications, AIE materials should be responsive to external stimulus, resulting in a change in their luminescent properties. It is also an important prerequisite for RTP materials to achieve these applications. Recently, various stimuli-responsive AIEgens have been developed [35]. For example, AIEgens with mechanochromic properties are ideal candidate materials for encryption application [36,37]. To obtain higher signal change, an AIEgen with a force-trigger photoluminescence property was also investigated [38]. Obviously, AIEgens with multi-stimuli-responsive and reversible fluorescence switching facilitate the designs for advanced encryption applications [39–41]. Herein, several kinds of AIE materials for information encryption and anti-counterfeiting are summarized.

2.1. AIEgens

Tetraphenylethene (TPE) is one of the mostly used AIE molecules, which exhibits bright blue luminescence under UV irradiation in the aggregated state. In this review, many AIEgens containing the TPE structure are present in various forms, such as TPE itself, TPE salts, and TPE derivatives. By linking two sulfonate spiropyrans with one TPE covalently, Liu and coworkers prepared an AIE–active orange–red/blue switch with photochromism property, sulfonate spiropyran–TPE–sulfonate spiropyran (STS) [42]. The STS can response not only to the acid/base stimulation, but also to the light irradiation and heating. Visible light irradiation could transfer orange–red STS into its ring-closed form, RSTRS, and the emission was consequently converted into blue. Both these forms exhibit obvious AIE characteristics. Through incorporating STS into polyvinylpyrrolidone matrix, advanced information encryption was investigated. A 0.5% volume fraction of nonvolatile sulfuric acid (0.5%) could stabilize the AIEgen in the STS form, while the AIEgen treated with a 0.02% volume fraction of acid would be in the STS form, but light irradiation could convert it into the blue emissive RSTRS. Combined with the nonfluorescent red dye, three levels of date encryption ("337", "377", and "71") could be simply achieved (Figure 1A).

In addition to being a light-, heat-, acid/base-responsive material, the mechanoresponsive AIEgen is also suitable for anti-counterfeiting and information encryption. By combing the spiro[fluorene-9,90-xanthene] and 9,9-dimethyl-9,10-dihydroacridine, Guo at al. prepared an AIE-active molecule (SFX-Ad) [43]. The SFX-Ad displays mechanoresponsive properties, and an obvious enhancement of the luminescence is companied with the crystal-to-amorphous transition. Based on this characteristic, the SFX-Ad is similar to the non-emissive Na_2CO_3, no matter under UV or visible light. However, after the grinding treatment, the emission enhancement of SFX-Ad supplied true information, and thus the anti-counterfeiting and information encryption could be easily realized.
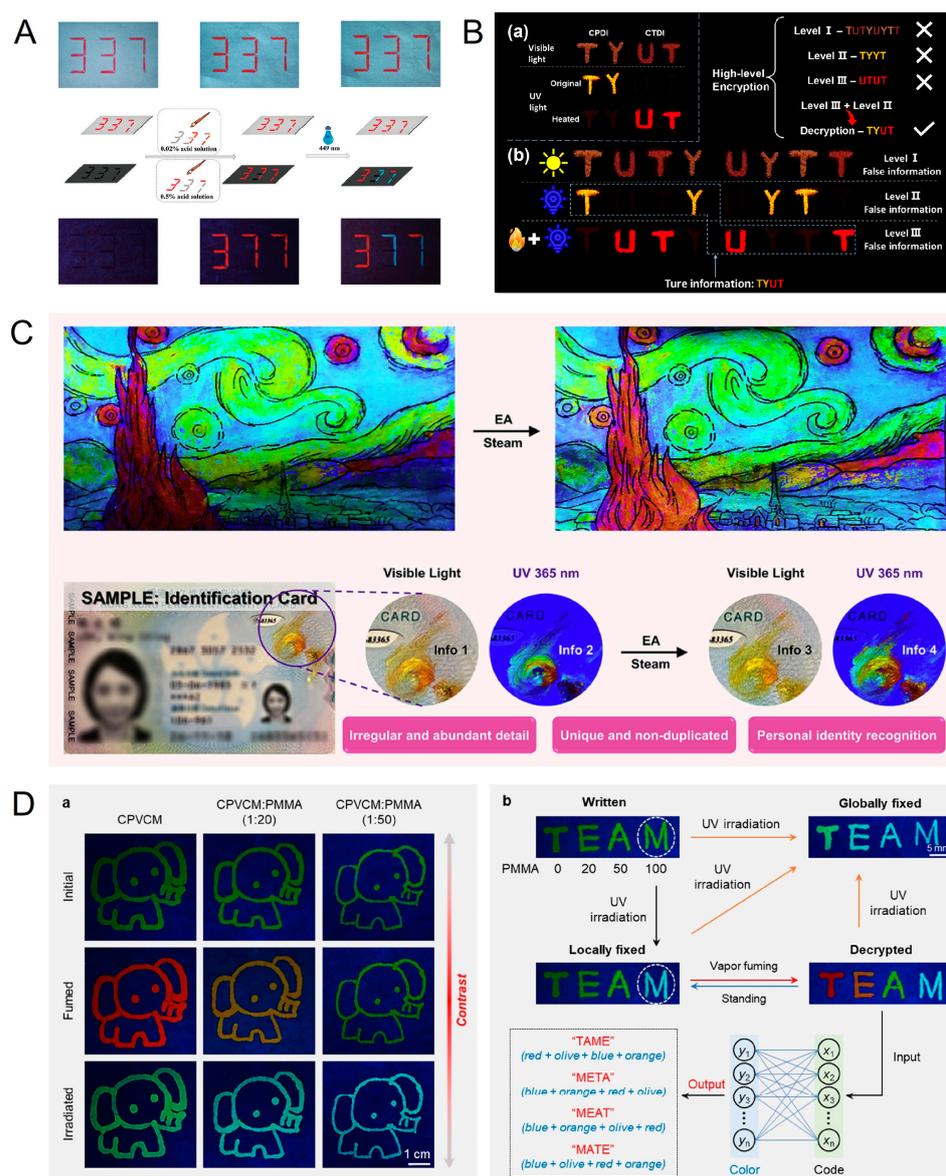
Figure 1. AIEgens based information encryption and anti-counterfeiting. (**A**) Light irradiation and acid triggered three levels of date encryption by the STS-RSTRS system [42]. Copyright 2021, with permission of The Royal Society of Chemistry. (**B**) The AIEgen CPDI and ACQ molecule CTDI based on fourth-level information encryption [44]. (**a**) Fluorescent images of the CPDI and CTDI based patterns under 365 nm irradiation. (**b**) Thermo-responsive fluorescent images for deep-hiding information under daylight and 365 nm irradiation. Copyright 2023, with permission from Elsevier. (**C**) Photographs of the "Starry Night" and identification card that was painted or hallmarked by the crystals of TPE-B, TPE-G, TPE-Y, and TPE-R with random force and deal with EA [45]. Copyright 2023, with permission from Elsevier. (**D**) Multicolor encryption based on CPVCM security ink [46]. (**a**) Fluorescent images of the initial sensors with an "elephant" image painted from the CPVCM (1 mM) security ink. (**b**) Multicolor encryption based on CPVCM (1 mM) security ink. Copyright 2023 Wiley.

By tailoring the π-bridge, Guo and coworkers regulated the luminescent behaviors of two carbazole derivatives, CPDI and CTDI [44]. The phenyl π-bridge of CPDI led to an AIE characteristic accompanied by thermally stimulated emission turn-off. The thienyl π-bridge of CTDI led to an ACQ characteristic accompanied with thermally stimulated emission turn-on. By using UV-light irradiation and thermal treatment as two sequential

keys, fourth-level information encryption was realized by combining these two molecules, AIE and ACQ (Figure 1B).

To achieve more color adjustments, a group of full-color-tunable AIEgens with mechanofluorochromic property were prepared by Tang and coworkers [45]. By adjusting the electron-withdrawing ability of the acceptors in the D-π-A structure, a broad emission spectrum was achieved. The emission wavelength could be from 460 to 640 nm by simply increasing grind time or variating the degree of the grind. The emission was mainly dependent on the packing morphologies of the molecules in the crystals. In addition, the ethyl acetate (EA) steam treatment could lead to the recrystallization of the ground compounds accompanied with a blue shift in the luminescence. Based on this property, these AIEgens were used for the design of 4D code, which has advantages such as strong fault tolerance and high reliability. Furthermore, the random grinding degree was used to prevent counterfeiting and avoid duplication. To investigate the anti-counterfeiting applications of these AIEgens, a figure of "Starry Night" was prepared with these colorful AIEgens with random forces. Obviously, the color and luminescence information in this figure is difficult to forge. The blue shifted color and emission of this figure after the treatment with EA further enhanced the level of the anti-counterfeiting. This design could also be used for the anti-counterfeiting of identification (ID) cards (Figure 1C).

If multicolor fluorescence changes could be achieved through a single luminogen, it would be easier to use it as an intelligent material. Tang and coworkers designed an AIEgen, (Z)-2-(5,5-dimethyl-3-(2-(4-oxo-4H-chromen-3-yl)-1-phenylvinyl)cyclohex-2-en-1-ylidene)malononitrile (CPVCM) [46]. Firstly, the CPVCM could react with primary amines through amination reaction, resulting in fast and reversible color change. Secondly, it could also respond to the UV irradiation through photoarrangement accompanied with a blue-shifted emission. By using a thin-layer chromatography plate as carrier, the multifunctional CPVCM was used for blue emissive information writing with UV lamp and mask. Then, the propylamine vapor treatment could change the surrounding into red and orange emission. At last, the UV irradiation could change the whole plate into blue emissive, and thus the information was erased easily. According to the different response model of the amination process and the photoarrangment, the authors further combined polymethyl methacrylate (PMMA) to regulate the degree of the amination process. In such case, the higher PMMA doping led to a weaker amination process and the corresponding red shift. A multicolor and advanced information encryption was realized (Figure 1D).

Another group of multiresponsive AIEgens, a series of 2-phenylazulene-1,1(8aH)-dicarbonitrile derivatives (DHAP-R, R=H, Br, Me, OMe, and NO_2), were also designed and prepared by Tang and coworkers [47]. The DHAP-R could response to both UV irradiation and heating, resulting in ring-opening (VHFP-R, non-emissive) and ring-closed (DHAP-R, emissive) form reversibly. Based on this characteristic, DHAP-Br and PMMA (1:2) were used for information storage. The UV irradiation induced date information could be erased by the heating, which was dependent on the temperature and time. The extraction and deletion of information is important for an excellent information encryption system. In this system, the decrypted information could be erased in a period at a specific temperature.

When time is introduced into the information encryption systems, there will be some new opportunities and designs for high-level security. By combing the cationic TPE derivative (TPE4N^{4+}) with the anionic spiropyran (ASP), which could be transformed from the fromsulfonato-merocyanine photoacid (SMEH) under the 420 nm light irradiation, Tang et al. reported a time-dependent information encryption system [48]. Once the ASP was formed, the electrostatic interactions between TPE4N^{4+} and ASP would lead to the restriction of the molecular rotation of the TPE, resulting in enhanced fluorescence emission. In such case, at the right time of UV irradiation, the true information could be decrypted. And after a period of dark condition, the emerged information would be erased, confirming an excellent self-erased property.

For the AIEgens, a simple change in a substituent or functional group might lead to a significant change in the properties of the molecule. Pu and coworkers obtained a group

of benzothiadiazole derivatives, which exhibited AIE characteristic and force-responsive fluorescence characteristic [49]. One exhibits red-shifted mechanofluorochromism behavior, and three exhibit blue-shifted mechanofluorochromism behavior, while another two do not response to the external mechanical stimulation. Based on this characteristic, multilevel information encryption was achieved easily.

Tetraphenylpyrazine (TPP) is also an important AIE structural unit and has various applications. To investigate its application in information storage, Chen and coworkers synthesized three AIEgens (TPP-o-py, TPP-m-py, TPP-p-py) with TPP as electronic donor to the acrylonitrile and pyridine as electronic acceptor [50]. These AIEgens exhibited a solvatochromic effect due to the twisted intramolecular transfer (TICT) effect, and they could response to the light and acid/base stimulus. With the silica gel plate as carrier, the reversible memory storage of the "JNU" could be achieved. In this process, the hydrochloric-acid-induced protonation effect transfers the AIEgens into a weak and red emission state; the triphenylamine could erase this information. Once the AIEgens on the silica gel plate were irradiated with the UV light, an irreversible memory storage of the "AIE" could be realized which was attributed to the photodimerization reaction.

2.2. AIEgens-Matrix Composite Materials

For the above AIEgens-based information encryption and anti-counterfeiting designs, the excellent stimuli-responsive property is essential. If some functional matrix is introduced, the common AIEgens could also be used for intelligent responsive materials. By combing the TPE and the widely used energy acceptor in the spectroanalysis, graphene oxide (GO), Chen and coworkers designed a composite material, TPE@GO, which showed switchable microstructure and corresponding fluorescence [51]. The main working principle was as follows: Firstly, the TPE@GO was non-emissive duo to the fluorescence quenching capability of the GO through fluorescence resonance energy transfer. Once the THF/H_2O mixture (V_{THF} = 60%, with the higher fluorescence enhancement) was added, the TPE was dissolved in the THF and then aggregated into nanoparticles after the volatilization of H_2O. In such a state, the blue emission of the TPE was recovered, and the information could be decrypted. While the formed TPE nanoparticles were further sprayed with pure THF, the TPE nanoparticles were dissolved and again accompanied with the information encryption. Based on this mechanism, the authors designed advanced information encryption with this TPE@GO functional material (Figure 2A).

Different to the regulation of luminescence with different water fraction, Zhang et al. designed a series of AIE-active freeze-tolerant hydrogels [52]. The freezing temperatures (Tf) could be regulated by the betaine concentration, and once the temperature was lower than the Tf of the AIE-active hydrogels, the luminescence of the AIEgen, $2,2',2'',2'''$-((ethane-1,1,2,2-tetrakis(benzene-4,1-diyl)) tetrakis-(oxy)) tetraacetate ($TPE-4CO_2Na$) would turn on. Based on this temperature-dependent luminescent property, this hydrogel was used for information encryption. Furthermore, the authors achieved the in situ sulfidation of Cu_2O nanparticles into Cu_9S_8 nanoparticles, which exhibited excellent photothermal property. Combined with the near infrared light response, advanced information encryption could be achieved easily, and part of the luminescence around the Cu_9S_8 nanoparticles could be selectively erased. Thanks to the decrypted information being irreversibly sensitive to temperature fluctuation, these hydrogels could be used for the real-time monitoring of cryopreserved biosamples during cold-chain transportation.

In a similar way, Min and coworkers designed and prepared a functional composite phase change fiber containing the pyrene-based AIEgens (Py-CH) through electrospinning technology [53]. Accompanied with the increased temperature from 30 to 160 °C, the fluorescence of the Py-CH showed a blue shift from the green-yellow to purple. Combined with the excellent latent heat and stability to thermal cycling, this fiber displayed potential applications in various fields in addition to anti-counterfeiting applications, such as solar energy conversation and storage, and high-temperature warning.

For thermoresponsive materials, high contrast ratio (CR) and fast and reversible thermoresponse were all attractive parameters. Li et al. synthesized a deep-red emissive squaraine-based AIEgen (TPE-SQ12) [54]. By dispersing this AIEgen into the elastomer, a thermal-responsive luminescent material was obtained. With the increased temperature, the free volume of elastomer was significantly expanded, resulting in the enhanced intramolecular movements of the AIEgens and the corresponding decreased luminescent intensity. Attributed to this thermal-responsive property, the authors achieved dual information encryption (Figure 2B).
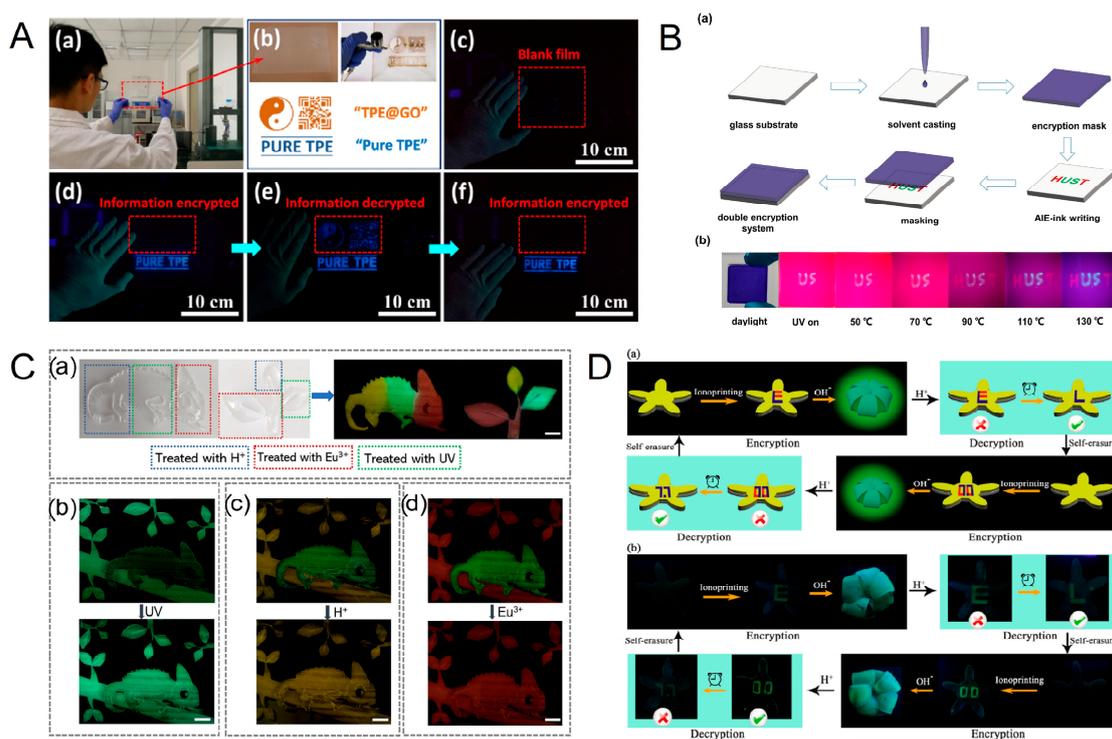

Figure 2. AIEgens-matrix composite-materials-based information encryption and anti-counterfeiting. (**A**) TPE@GO for reversible information encryption [51]. (**a**,**b**) Optical images of the plastic film on which "Tai Chi" and "QR code" patterns were sprayed with GO and TPE dispersions in turn, and "PURE TPE" pattern was sprayed with pure TPE dispersion. (**c**) Optical images of empty film under UV light. (**d**) Optical images of original sprayed film under UV light. (**e**) Optical images of sprayed film treated by THF/H$_2$O mixture under UV light. (**f**) Optical images of sprayed film treated by THF/H$_2$O mixture, and pure THF in turn under UV light. Copyright 2019 American Chemical Society. (**B**) Double encryption system based on SBR/TPE-SQ12 film [54]. (**a**) The fabrication process. (**b**) Photographs under daylight and irradiated 365 nm UV light at different temperatures. For AIE-ink writing, "H" and "T" are made of 27-TPA, while "U" and "S" are made of TPE-4N. Copyright 2022 Wiley-VCH GmbH. (**C**) The color changes of the self-healing hydrogel responsive to UV light, H$^+$, and Eu^{3+} [55]. (**a**) Images of multicolor luminescence display under different in situ stimuli. PVA–HCPB hydrogel that switches luminescence after (**b**) UV irradiation, (**c**) adding H$^+$, (**d**) adding Eu^{3+}. Copyright 2022, with permission of The Royal Society of Chemistry. (**D**) Three-dimensional multistage information encryption, decryption, and self-erasure processes based on the functional bilayer hydrogel [56]. (**a**) Schematic representation and (**b**) photographs of 3D multistage information encryption, decryption and self-erasure processes: the multistage information is loaded onto a 2D flower-shaped hydrogel and encrypted inside 3D hydrogel geometry during the SDFC change process. Right information (the letter "L" from the abbreviation of "love" and the date "7.7") would be decrypted at different stages. Copyright 2023, with permission of The Royal Society of Chemistry.
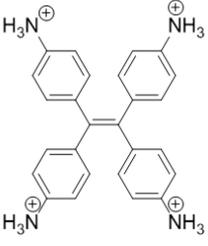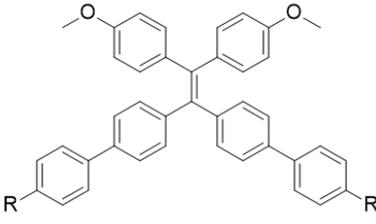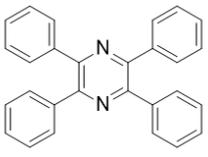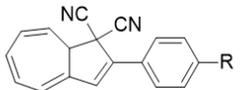
In order to endow the multi-responsive luminescent materials with self-healing capability, Jia and coworkers developed a self-healing hydrogel which exhibited multicolor luminescence

and could be responsive to three external stimulus, including UV light, acid, and Eu^{3+} [55]. Treatment with UV light would lead to a green emission, and treatment with acid would lead to a yellow emission. Eu^{3+} would lead to red luminescence, which was attributed to the coordination between the Eu^{3+} and the carboxyl. The UV light triggered emission enhancement could be recovered, so this hydrogel could be used for reversible information encryption and decryption. Based on this multi-responsive property, a multicolor chameleon-shaped hydrogel could be obtained and a sequential color change from green to yellow could be achieved through adding acid to the UV-irradiation-triggered green emissive chameleon-shaped hydrogel. Furthermore, the sequential color change from green to red could be simply achieved by the addition of Eu^{3+} to the green emissive chameleon-shaped hydrogel (Figure 2C).

Endowing the multi-responsive luminescent materials with shape recovery capability is another interesting design for intelligent materials. Tang et al. developed a functional bilayer hydrogel with synergistic deformation and fluorescence color (SDFC) change property [56]. The fluorescence enhancement was attributed to the pH-driven aggregation of the AIEgens, and electrostatic interaction and dynamic covalent bonds also contributed to the aggregation. Based on this fluorescence regulation strategy, 2D information encryption could be easily realized. Together with the pH-triggered deformation capability, a sequential 3D multistage information encryption, decryption, and self-erasure process could be achieved (Figure 2D), which was of typical advanced information encryption design and exhibited larger information storage capacities.

All the forms of the TPE and TPE derivatives, and some other AIE structures cited in this review, for example the tetraphenylpyrazine, are summarized in Table 1.

Table 1. The basic structures of the AIEgens in the citations.

Structural Classification	Representativeness Structural Formula	References
Tetraphenylethylene (TPE)		[50]
TPE salts		[47,51,55]
TPE derivatives		[41,44,53]
Tetraphenylpyrazine (TPP)		[49]
Others		[42,43,45,46,48,52,54]

2.3. AIE Carbon Dots

Usually, AIEgens refer to the organic molecules that exhibit AIE property. Various nanomaterials, such as metal clusters and carbon dots (CDs), have already exhibited typical AIE property and could be regarded as functional AIEgens. Recently, many AIE CDs have been prepared and used for anti-counterfeiting and information encryption applications.

The hydrothermal method is one of the most widely used methods for preparation of CDs. By this simple method, Wang and coworkers synthesized blue-emissive CDs with a quantum yield of 7.6% in aqueous state and 29.2% in solid state [57]. Thus, the CDs exhibited classical AIE property due to the functionalization by Na^+, and their emission color turned to cyan in solid state, which was attributed to the surface state change caused by aggregation. Based on these characteristics, the authors used these CDs for anti-counterfeiting designs. An image of waxberry on a filter paper was printed with the security inks composed of the CDs. Under 365 nm UV lamp, the waxberry showed cyan emission and blue emission once being wet by water. In addition, this security inks could also be used for the printing of various text and patterns (Figure 3A).
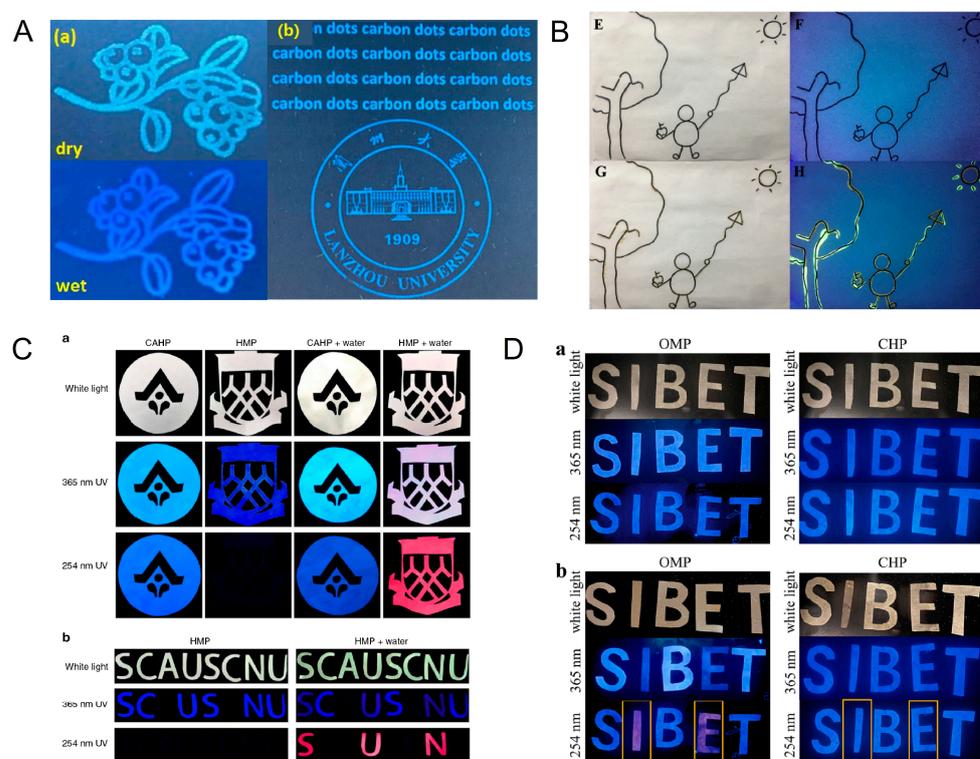

Figure 3. AIE carbon-dots-based information encryption and anti-counterfeiting. (**A**) Na^+ functionalized CDs for anti-counterfeiting and printing [57]. (**a**) CDs for anti-counterfeiting. (**b**) CDs for printing fluorescent image and text. Copyright 2021, with permission from Elsevier. (**B**) Acid-sensitive multi-color AIE CDs for advanced information encryption [58]. Photographs of the information encryption which drawing by Y-AIE-CDs and O-AIE-CDs fluorescent inks under (**E**) sunlight and (**F**) 365 nm UV lamp. Photographs of the information encryption which drawing by Y-AIE-CDs and O-AIE-CDs fluorescent inks under (**G**) sunlight after being wet with sulfuric acid solution (pH = 1) and (**H**) 365 nm UV lamp after being wet with sulfuric acid solution (pH = 1). Copyright 2022, with permission from Elsevier. (**C**) Hydrophobic AIE CDs for advanced anti-counterfeiting and dual-encryption applications [59]. (**a**) H-CD as-prepared solution-filled mark pen (HMP) utilized as an anti-counterfeiting badge compared with commercially available highlighter pen (CAHP). (**b**) HMP utilized as a dual-encryption badge. H-CD, hydrophobic carbon dot. Copyright 2019 Nature Publishing Group. (**D**) Water-sensitive CDs for information encryption [60]. (**a**) Encryption effect without adding water. (**b**) Encryption effect after adding water, and only the letters "I" and "E" was treated with water. Copyright 2022, with permission from Elsevier.

To develop multi-color anti-counterfeiting and information encryption technologies, the multi-color AIE CDs were prepared by Gao and coworkers [58]. By using crystal violet as the precursor, four AIE CDs with different emission colors (B-AIE-CDs, G-AIE-CDs, Y-AIE-CDs, and O-AIE-CDs) were synthesized. The sulfuric acid concentrations, temperatures, and reaction times played important roles, but the concentration of the sulfuric acid was the most important factor due to its function in regulation of the carbonization degree and the type and content of nitrogen. Combined with the acid-sensitive property of partial of these AIE CDs, the applications for anti-counterfeiting and information encryption were investigated. Firstly, the acid-triggered orange fluorescence of the real password could be clearly distinguished from the false password, which showed other fluorescence. In addition, the acid-triggered decryption of the hidden information "123456789" displayed the excellent information encryption capability of these multi-color CDs (Figure 3B).

Through the simple one-pot solvothermal method, Hu et al. synthesized a type of functional hydrophobic CDs, which exhibited blue emission in the dispersed state and red emission in the aggregated state [59]. The water could induce the aggregation of the hydrophobic CDs, leading to π-π stacking interactions of the carbonized cores and the accompanied red emission. The AIE property might be from the restriction of the surfaces' intramolecular rotation around disulfide bonds. Interestingly, the blue-red emission change is reversible by the regulation between the dissolved and aggregated state. The authors used this AIE CDs as luminescence ink for advanced anti-counterfeiting and dual-encryption applications. The blue emission of the pattern from the commercially available highlighter pen was almost stable after the water treatment, no matter whether under 365 nm or 254 nm irradiation. However, the blue emission of the pattern from the luminescent ink of this hydrophobic CDs turned to pink under 365 nm irradiation, and turned to red emission under 254 nm irradiation. Obviously, this could be used for high-level security and anti-counterfeiting. Combined with wax sealing, this luminescent ink could be used for multilevel information encryption. Because the "C", "S", and "U" were covered with wax, their emission was no longer sensitive to the water treatment; only the bare "S", "U", and "N" showed red emission under 254 nm irradiation, showing the true information (Figure 3C).

Similarly, by using dithiosalicylic acid and precursors containing amino groups, Wang and coworkers also prepared CDs that exhibited AIE property and dual-emission in different states [60]; the dual-emission regulation was also reversible. When these CDs were used for information encryption, the water treatment could lead to orange emission from the initial blue emission under 254 nm irradiation, while the emission of the words written by the commercially available highlighter pen showed no obvious changes (Figure 3D).

3. Application of the RTP Materials in the Information Encryption and Anti-Counterfeiting

Time-resolved spectral imaging is an ideal technology for high-level encryption and anti-counterfeiting. Among the luminescent materials with time-resolved ability, RTP materials, especially the purely organic ones [61–64], have been a topic of keen interest in various applications. Recently, several organic RTP materials that emit bright red emission have been developed and exhibited potential applications in bioimaging [65–67]. Obviously, these RTP materials could also expand and enrich the design choices of anti-counterfeiting and information encryption. Although all kinds of RTP materials, including inorganic ones, organic ones, and even organic-doped inorganic ones, could be used for information encryption and anti-counterfeiting, stimuli-responsive organic RTP materials were better choices due to their significant signal changes [68,69]. In addition, some new constructing strategies, for example through manipulating intermolecular interactions, could not only enrich the variety of RTP materials, but also supply many design choices for stimuli-responsive RTP materials [70,71]. Herein, the RTP molecules, RTP molecules-matrix composite materials, and phosphorescent-CDs-based information encryption and anti-counterfeiting designs are summarized.

3.1. RTP Molecular Systems

Recently, the host–guest doping method has proven to be an efficient route to construct RTP materials with long lifetime, high quantum, and various wavelengths [72–75]. By using triphenylphosphine and triphenylarsenic as the guest and a series of triphenylamine derivatives as host, Dong et al. synthesized a range of RTP materials with multi-color emission [76]. The RTP emission could be effective in a wide range of host–guest ratios from 50:1 to 20,000:1, and could be even much wider. In these systems, the host molecules could provide a rigid environment, which avoided the quenching of the triplet excitons by oxygen. These RTP systems were sensitive to temperature because of the temperature regulated vibrational freedoms of the host–guest systems. The authors successfully used these temperature-sensitive RTP materials for multilevel thermochromic anti-counterfeiting.

Similarly, Dong and coworkers also prepared a series of RTP materials through the host–guest doping method [77]. Herein, the host molecules played the role of the bridge to enhance the intersystem crossing and rigid environment to limit the nonradiative decay of the triplet excitons. One of the optical systems, TPA-FL-CN/CBN, exhibited a phosphorescence lifetime of 847 ms and quantum yield of 4.7%. Based on these RTP systems, the authors developed phosphorescence encryption and decryption applications. By using the FL-2CN/ABN ethyl acetate as the phosphorescence ink, dragonflies and the dandelions patterns could be hidden under 365 nm UV irradiation or under ambient light. However, after removing the UV irradiation, these patterns with yellow phosphorescence could be decrypted easily. Furthermore, the RGB color value at different times could be used as secret keys in phosphorescence encryption system (Figure 4A).

The energy transfer process can enrich the fluorescence emission wavelengths and application designs of the RTP materials [78–81]. Yang and coworkers designed and synthesized a range of host–guest RTP systems based on several asymmetric diarylamine guests [82]. Firstly, they investigated the multi-stimulus-responsive properties of these materials. Further applications of these RTP systems for anti-counterfeiting were explored based on the time resolved characteristic of the MDPA-Ph@DMAP system and energy transfer. For the RTP system only, the green RTP emission of the badge pattern and words could be observed after removing the UV irradiation. However, if the rhodamine B was added into the RTP system, a pink emission was observed under UV irradiation. After removing UV irradiation, the emission turned a green and pink color, the latter being attributed to the emission of the rhodamine B, resulting from the energy transfer from the green RTP emission (Figure 4B).

With the development of the host–guest RTP materials, there is still a challenge in effective matching between the host and guest molecules for the efficient intersystem crossing. Up to now, the trial-and-error method is still widely used. To better predict the host molecules for matching the guest RTP emitters, Liu et al. provided a simple descriptor ΔE based on the intersystem crossing via higher excited states mechanism [83]. According to this descriptor, they predicted five commercially available host components to pair with naphthalimide and naphtho[2,3-c]furan-1,3-dione emitters. Interestingly, the accuracy of this prediction was as high as 83%. This was an important exploration for the further development of the host–guest RTP materials. Based on the developed RTP systems with different lifetimes and wavelengths, the authors investigated their anti-counterfeiting applications, which exhibited classical time-resolved characteristic.

Another important host–guest interaction is the complexation between the supramolecular macrocyclic hosts and the guests, for example the crown ethers and the K^+. Tang and coworkers first reported ultralong RTP emission from traditional crown ethers [84]; the RTP lifetime from the crown ethers could be effectively prolonged through interaction with the K^+. In such cases, the invisible RTP could be changed into a visible RTP, which was suitable for the information encryption and decryption. Based on this newly discovered smart luminescence system, an advanced encryption application was designed. Firstly, an encryption pattern of "8" was printed with functional ink containing different components of the dyes, the B15C15 crown esters, and K^+. Upon 254 nm irradiation, all parts of the "8" were emissive attributed to the dyes. After removing the UV irradiation, only the pre-activated part in the "7" with K^+

was visible. Once sprayed with a solution of K$^+$, the parts containing B15C15 in the pattern of "3" could be seen clearly (Figure 4C). As a result, a multilevel encryption was achieved.

In addition to the host–guest RTP systems, single-component RTP emitters were also widely studied and applied, including in anti-counterfeiting and information encryption. Through a molecular design strategy, Zhao et al. explored the photoactivated persistent RTP behaviors of a series of triphenylphosphine oxide derivatives [85]. The photoactivation speeds and emission decay times of these materials could be regulated by the change of the substituent groups. In addition, the different RTP emission behaviors were attributed to the molecular stacking modes. By choosing three RTP systems, FPPO, MeOPPO, and TMeOPPO, an application of multilevel information encryption was investigated. At first, after removing the UV irradiation, only the green RTP of the small house was visible. Upon irradiation at 300 nm for 1 min, the MeOPPO was activated and exhibited a prolonged lifetime. When the photoirradiation time was changed to 20 min, all the patterns could be activated. This three-level encryption could effectively enhance the security level (Figure 4D). Further, the authors also designed an anti-counterfeiting application based on the thermochromic RTP behaviors of these materials, which also exhibited great potential for visual detection of temperature.
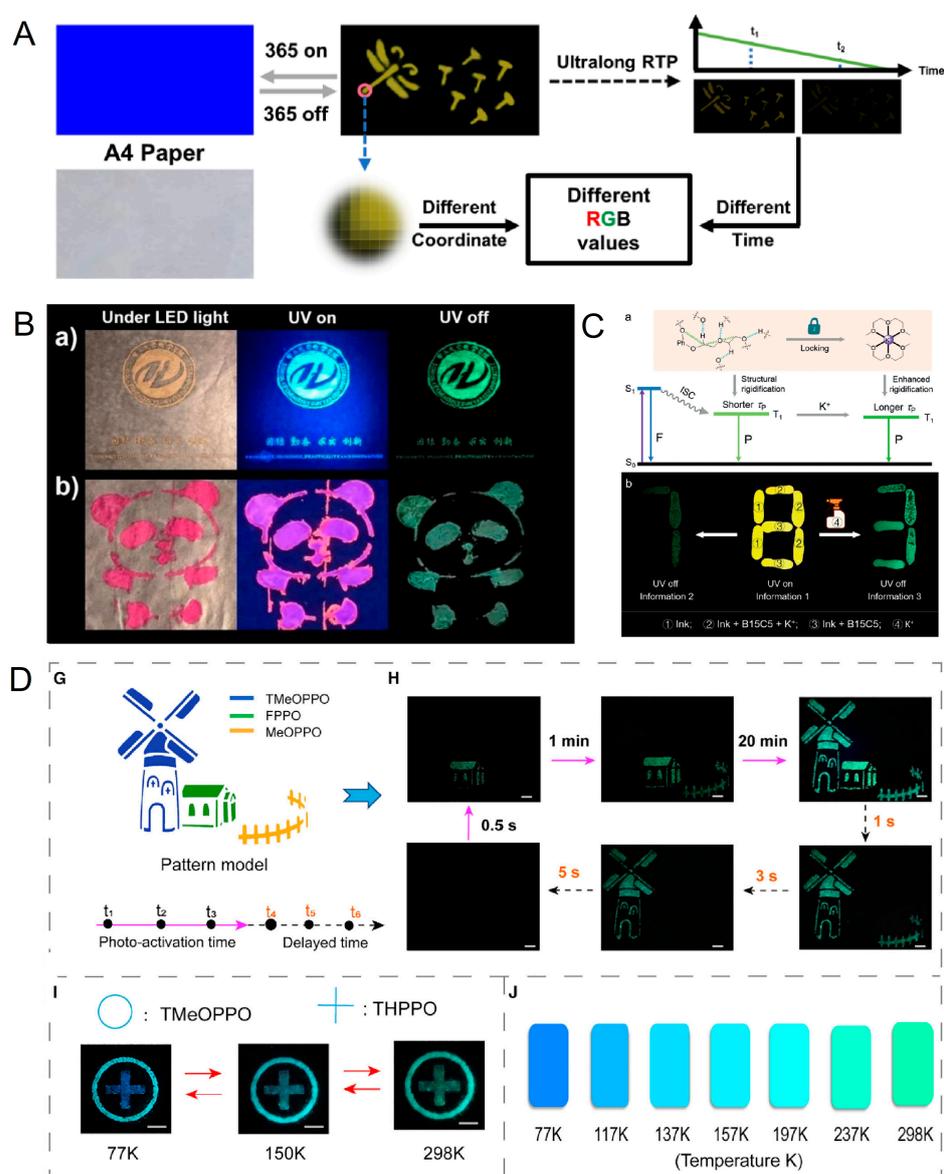

Figure 4. RTP molecular systems-based information encryption and anti-counterfeiting. (**A**) FL-2CN/ABN ethyl acetate ink for information encryption and the RGB-value-based high-level encryption [77]. Copyright

2021, with permission from Elsevier. (**B**) The MDPA-Ph@DMAP system and energy-transfer-based anti-counterfeiting application [82]. (**a**) Anti-counterfeiting application of the pattern of department emblem and the motto. (**b**) Anti-counterfeiting application of the "panda" pattern with a third component rhodamine B doping. Copyright 2023, with permission of The Royal Society of Chemistry. (**C**) RTP from the crown ethers and K$^+$ for deep information encryption [84]. (**a**) Theoretical models based on Jablonski diagram for understanding the performance of crown ether-based tunable RTP in the solid state. The green and cyan dashed line indicates C⋯O and hydrogen bonding interactions, respectively. F and P indicates fluorescent and phosphorescent luminescence, respectively. (**b**) Photograph shows advanced-encryption application based on K$^+$ "activated" persistent phosphorescence strategy. Copyright 2020 Wiley-VCH GmbH. (**D**) Triphenylphosphine oxide derivatives with photoactivated persistent RTP behaviors for multilevel information encryption, anti-counterfeiting, and temperature sensing applications [85]. (**G**) Demonstration of anti-counterfeiting label using different phosphors. (**H**) Multiple anti-counterfeiting applications by using MeOPPO, FPPO, and TMeOPPO. With photoactivation time changes, different information can be captured by the naked eye. Scale bars, 1 cm. (**I,J**). Temperature-dependent color chart show the ability of THPPO crystal inmulticolor displays and visual sensing of temperature. Scale bars, 1 cm. Copyright 2021, with permission from Elsevier.

Recently, Ge at al. reported triphenylmethylamine-based single-component phosphors that emitted color-tunable ultralong RTP [86]. Under UV irradiation of different wavelengths, the RTP emission ranged from cyan to orange. This characteristic was used for high-level anti-counterfeiting. In addition, due to the high sensitivity of this material, UV light ranging from 350 to 370 nm could be detected in a minimal interval of 2 nm.

3.2. RTP Molecules-Matrix Composite Materials

To reduce the nonradiative relaxation induced quenching of the triplet state, crystallization was a usually adopted method to construct RTP materials. Many efforts have been made to pursue RTP materials without the crystallization process. Among these explorations, a simple method of radical binary copolymerization of acrylamide and different phosphors was developed by Tian et al. [87]. Through this method, the phosphors could be effectively immobilized with the formed rigid polymer matrix. Further, the hydrogen bond cross-linking between the polymeric chains could also enhance the rigidity of the luminescence polymers. The authors used this easily prepared amorphous RTP materials for encryption ink. In dry state, the pattern written by this ink showed obvious RTP emission, while the wetting treatment could lead to the hiding of this information.

Similarly, Zhao et al. also designed a strategy to construct amorphous RTP materials [88]. To achieve the embedding of molecular phosphors into the rigid polymer matrices, they used poly (vinyl alcohol) (PVA) as the matrix and hexa-(4-carboxyl-phenoxy)-cyclotriphosphazene as the guest molecule. The nonradiative relaxation of the triplet excitations could be effectively suppressed. Firstly, the diffusional motions of the composite material could be reduced by the strong interaction formed by the hydrogen bonds between the guest and matrix. Secondly, the hydrogen bonds between guest molecules were useful for the promotion of the intersystem crossing processes and the restriction of the vibration. In such case, an RTP film with long lifetimes (up to 0.75 s) and high phosphorescent quantum yields (11.23%) was obtained; this strategy was proven to be suitable for some other molecules. This RTP material with PVA matrix showed excellent application potentials in anti-counterfeiting and security. In addition to normal security based on afterglow emission, the water in the air induced the quenching of RTP via breaking of the hydrogen bonds, which enriched the revisable design for advanced anti-counterfeiting.

Attributed to strong hydrogen bonding with PVA matrix, a series of vanilla-derivatives-based RTP polymers were reported by Zhao et al. [89]. These polymers exhibited ultralong RTP emission under ambient condition, and the longest lifetime could be up to 7 s from the methyl vanillate-PVA composite materials. In addition, the vanilla-doped PVA films showed temperature-dependent phosphorescence, which should be attributed to water-

related hydrogen bonds breakage and reformation. The authors explored the security ink application of these luminescent materials. The invisible information on a postcard could be visible after the UV-irradiation-triggered phosphorescence emission. The temperature-dependent RTP emission and quenching showed high reversibility in 50 circles of repeated temperature changes between 0 and 65 °C (Figure 5A). The functional ink could be refilled in the pen and this process was highly feasible and reproducible.

In addition to the above temperature-dependent RTP intensity, the smart PVA functionalized RTP materials with temperature-tunable emission colors were also attractive. Xu et al. prepared two RTP materials with two indolocarbazole derivatives, IaCzA and IbCzA, by using PVA as the matrix [90]. The IbCzA-doped PVA film exhibited intense blue RTP with an excellent phosphorescence quantum yield of 19.8% and long lifetime of 1.8 s. Combined with the fluorescence dye and the temperature sensitivity of the RTP color, a high-level anti-counterfeiting and information encryption application was designed. The parts composed of IaCzE-0.1 %-PVA in the patterns exhibited blue fluorescence which showed up in the dark gray and gray parts, which was no longer visible after removing the UV irradiation. In such case, the pattern of "blooming deep-blue rose" was seen when the UV irradiation was on. However, the parts composed of IbCzA-0.1 %-PVA could still be visible as "rosebud" when the irradiation was off. In addition, the emission color of the rose could be tuned by changing the temperature; it gradually changed to green when the temperature was changed from 28 to 0 °C, and this process was reversible. This ink was also used for temperature-controlled information encryption.

Cucurbit[7]uril (CB[7]) has also proved to be an effective matrix for amorphous RTP materials. Liu et al. prepared a series of RTP materials with CB[7] and acrylamidephenylpyridium copolymers with various substituent groups (P-R: R=-CN, -CO$_2$Et, -Me, -CF$_3$) [91]. These RTP materials exhibited second-level RTP emission with lifetimes from 0.9 to 2.2 s. By introducing the energy acceptors, such as the organic dyes Eosin Y and SR101, room temperature afterglow (RTA) materials were successfully synthesized with yellow (568 nm) and red (620 nm) emission. With the increased ratio of the energy acceptors, the lifetimes of the RTA emission turned shorter. Based on these characteristics, the authors designed anti-counterfeiting and encryption applications. Time-resolved information reading could be achieved with a combination of RTP and RTA materials. The long lifetime of RTP materials could lead to controllable presentation of effective information after the removal of the UV irradiation, such as the green lotus, the "Me", and the tree. The RTA materials with longer wavelengths could enrich the color of the patterns under the UV irradiation and a short time after the removal of the UV irradiation. In addition, with the different choices in RTP materials, time-resolved information could also be easily achieved (Figure 5B).

In the above research, an introduced matrix, such as PVA and cucurbit uril, is mainly used as the rigid environment to enhance RTP emission. The introduced matrix could also be used for the regulation of RTP emission or introducing stimulus-responsive attributes. Gao and coworkers constructed temperature-sensitive RTP materials based on a new strategy of molecular thermal motion modulated RTP emission [92]. Most of the stimulus-responsive host–guest RTP systems were based on the reduction in the distances between the two components, resulting in the RTP emission turning on. Until now, there have been rare effective methods to enlarge the distances between the two components leading to the reduction and turning off of the emission. By combining the usual chromatographic separation method with ubiquitous molecular thermal motion, the authors achieved the separation of the hosts and guests, accompanied by the quenching of the RTP emission. All the normal silica gel, reverse silica gel, and neutral silica oxide could be used as the separation matrix, and the regulation efficiency was determined by the chromatographic separation efficiency of the matrix. Experimental characterization, such as nuclear magnetic resonance spectroscopy, mass spectrometry, X-ray diffraction spectroscopy, together with the calculation of Gibbs free energy by Gaussian simulation, all confirmed that the quenching mechanism was attributed to the separation of the hosts and guests. This newly constructed stimulus-responsive RTP material was used for multilevel encryption applications. Firstly, with the abundant

host–guest RTP systems, a six-level temperature-responsive encryption was achieved easily. Secondly, decryption of valid messages triggered by specific temperatures further expanded the design choices of this material. Thirdly, combined with the RTP systems with different colors and responsive temperatures, thermochromic RTP materials for advanced information encryption could be realized, resulting in the scene of "the resurrection of withered flowers". At last, the detection of the cold chain break could also be achieved due to the wide responsive range of temperature, from high temperature to room temperature and then to refrigerated temperature (Figure 5C).

Figure 5. RTP molecules-matrix composite-materials-based information encryption and anti-counterfeiting. (**A**) Vanilla derivatives-PVA composite RTP ink for encryption and decryption [89]. Copyright 2021 Exclusive Licensee American Association for the Advancement of Science, distributed under a Creative Commons Attribution NonCommercial License 4.0 (CC BY-NC). (**b**) Sensitive anticounterfeiting on a postcard after turning off 254 nm light. (**d**) Photos of ink-brushed leaf pattern on glazed printing paper, showing temperature-dependent changes between room temperature (RT) and 65 °C for 50 times. Bright blue fluorescence emits when turning on the 254 nm UV lamp, and cobalt phosphorescence emission is observed when turning off the 254 nm UV lamp. (**e**) A hand-painted lotus flower pattern with M1-acid-0.3 mg PVA ink showing cobalt phosphorescence emission after heating treatment (65 °C) and turning of the UV light. (**B**) RTP materials from cucurbit[7]uril and acrylamidephenylpyridium copolymersm, together with some energy transfer composites, for anti-counterfeiting and information encryption [90]. (**a**) The lotus colored by various supramolecular polymers and ternary supramolecular systems before and

after excited by 254 nm ultraviolet lamp (1, 2, 3 and 4 represented P-CF$_3$/CB[7], PH-1/CB[7]-3%EY, PCO$_2$Et/CB[7]-5%SR101 and P-CO$_2$Et/CB[7], respectively). (**b**) The schematic illustration of triplet digit encryption fabricated by supramolecular polymers PBr-1/CB[7], P-CN/CB[7] and P-CO$_2$Et/CB[7] (Light source: 254 nm ultraviolet lamp). (**c**) The words "Merry Christmas" written by supramolecular polymers and ternary supramolecular system before and after ignited by 254 nm ultraviolet lamp (1, 2, 3, 4 and 5 represented P-CF$_3$/CB[7], P-CO$_2$Et/CB[7]-7%SR101, P-CO$_2$Et/CB[7]-3%SR101, PH-1/CB[7]-3%EY and P-CO$_2$Et/CB[7], respectively). Copyright 2022 Wiley-VCH GmbH. (**C**) Molecular thermal motion modulated RTP for multilevel information encryption and detection of cold chain break [92]. (**a**) Six-level information encryption application of the thermal-responsive RTP systems (component 1 for rhodamine B & silica-OH, 2 for TPB & silica-OH, 3 for NA/ABDO & silica-OH (1:10), 4 for TPB/TPP & silica-OH (1:10), 5 for NA/ABDO & silica-OH (1:1), 6 for TPB/TPP & silica-OR (1:3), 7 for NA/DCB & silica-OH (1:1), and 8 for TPB/TPP & NaCl (1:5)). (**b**) Information encryption "QR code" constructed by NA/DCB system and three different matrix (component 1 for NA/DCB & NaCl (1:5), 2 for NA/DCB & silica-OR (1:5), and 3 for NA/DCB & silica-OH (1:5). (**c**) The thermochromic RTP system for information encryption (component 1 for 2,3-NA/PCP & silica-OH (1:5)+Py/PCP & NaCl (1:5), 2 for NA/PCP & NaCl (1:20), and 3 for NA/PCP & silica-OH (1:5) +2,3-NA/PCP & NaCl). (**d**) Monitoring of two kinds of simulated cold chain break with two yellow and green RTP systems ("cold" for NA/ABDO & silica-OH (1:10) and "safe" for TPB/TPP & silica-OH (1:10)). Copyright 2022 Exclusive Licensee American Association for the Advancement of Science, distributed under a Creative Commons Attribution NonCommercial License 4.0 (CC BY-NC).

3.3. Phosphorescent Carbon Dots

PVA, which had been proven to be a universal matrix for constructing temperature-responsive RTP materials, was also successfully used for preparation of thermal-treatment-controlled RTP CDs/PVA composite materials [93]. Qu et al. embedded originally synthesized CDs (CD 1) or 200 °C thermal-treated CDs (CD 2) into the PVA matrix through post-synthetic thermal annealing at 200 or 150 °C. After annealing, both of these films showed phosphorescence. The control experiment with bare PVA film revealed that the luminescence was attributed to the embedded CDs. The CD 2 embedded PVA films showed visible phosphorescence after the annealing at 150 or 200 °C, while the CD 1 embedded films only showed phosphorescence after the annealing at 200 °C. According to these characteristics, multilevel encryption was realized. Under UV irradiation, all the information could be visible in the form of blue luminescence. However, only the first level of encryption "CD", which was written with the CD 2, could be seen after the annealing at 150 °C. All the CD 1- and CD 2-based information "CDots" showed green phosphorescence, which was the second level of information decryption (Figure 6A).
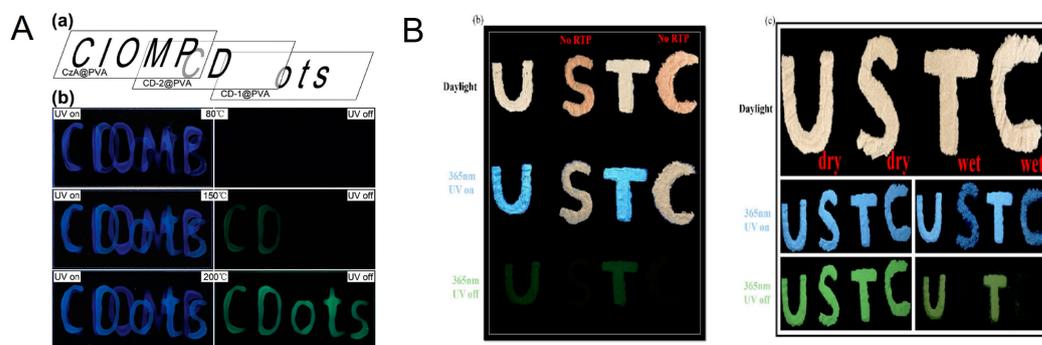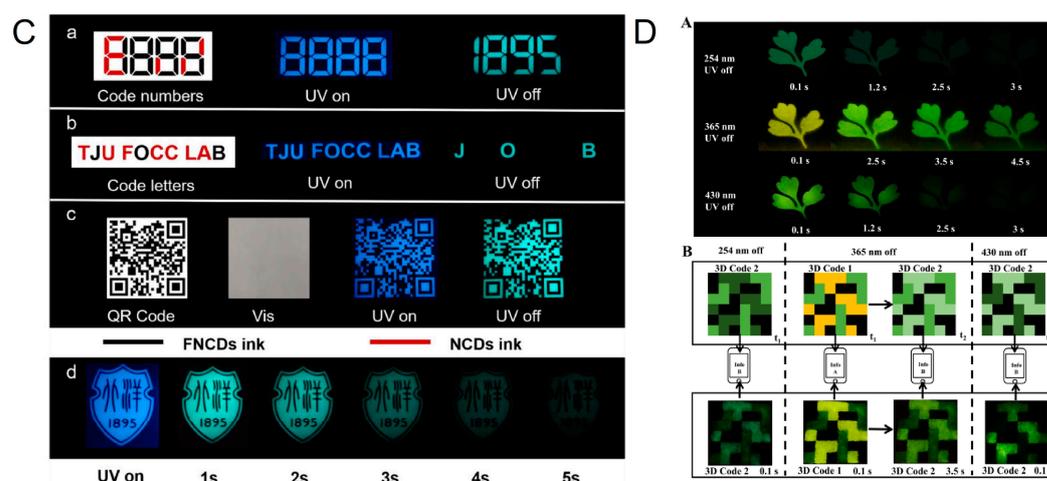

Figure 6. *Cont.*

Figure 6. Phosphorescent-carbon-dots-based information encryption and anti-counterfeiting. (**A**) Thermal-treatment controlled multilevel fluorescence/phosphorescence encryption with citrazinic acid (CzA@PVA), CD-1@PVA, and CD-2@PVA composites [93]. (**a**) Three overlapping patterns written with CzA@PVA ("CIOMP"), CD-2@PVA ("CD"), and CD-1@PVA ("ots") composite. (**b**) Photographs of the combined patterns realized with the mentioned three kinds of composites after annealing at 80, 150, and 200 °C (from top to bottom), under UV light excitation (left) and after switching UV light off (right). Copyright 2018 Wiley-VCH GmbH. (**B**) Boron doping phosphorescent CDs for anti-counterfeiting and information encryption [94]. (**b**) Anticounterfeiting application of PCD100. (**c**) Data encryption application of dry and wet PCD100. Copyright 2022, MDPI. (**C**) FNCDs and NCDs based information storage and anti-counterfeiting [95]. Printed images using (**a**) RTP FNCDs-based and (**b**) interference NCDs-based inks on commercial paper under a 365 nm UV lamp for on and off situation. (**c**) Images of anti-counterfeiting and information protection applications of the FNCDs (QR code under daylight, 365 nm UV lamp for on and off situations). (**d**) Digital images of school badge on filter paper printed using FNCDs ink, and irradiation with a 365 nm UV lamp for on and off situations. Copyright 2021, with permission from Elsevier. (**D**) Multilevel information encryption based on the CDs/Na$_{0.5}$Mg$_{0.25}$Cl with UV irradiation of different wavelengths [96]. (**A**) The phosphorescence photographs of CDs/Na$_{0.5}$Mg$_{0.25}$Cl after turning off the UV lamp (254, 365, and 430 nm) under air atmosphere. (**B**) Multilevel phosphorescence colored 3D codes for advanced dynamic information encryption. Copyright 2023 Wiley-VCH GmbH.

By a two-step hydrothermal process, Li et al. prepared a kind of phosphorescent CDs, which showed blue fluorescence and green phosphorescence [94]. During the synthesis process, Vitamin B1 was used as the raw material, and ethylenediamine was used as a passivator. After the first hydrothermal process, boric acid was used as a phosphorescent enhancer, which led to the enhanced intersystem crossing efficiency. The lifetime of the green phosphorescence was 293 ms, which could be used for simple time-resolved anti-counterfeiting together with blue fluorescence emission. With the assistance of non-phosphorescent material, the CDs could be used for higher level encryption by selectively turning on the phosphorescence of the "U" and "T". Furthermore, the stimulus-responsive property could enrich the design choices. For these CDs, the wetting treatment could also lead to the quenching of the phosphorescence of the "S" and "C" accompanied with the decreased blue fluorescence emission of these two letters (Figure 6B).

Through the fluorine-nitrogen co-doping strategy, Feng et al. synthesized a kind of CDs, which exhibited both fluorescence and phosphorescence emission. This CDs had an ultralong phosphorescence lifetime of 1.14 s, and also showed an excellent phosphorescence quantum yield of 8.3% [95]. Similarly, the co-doping of fluorine and nitrogen was achieved by the second hydrothermal process. By using a commercial inkjet printer, the fluorine and nitrogen co-doping CDs (FNCDS) and the nitrogen doping CDs (NCDS) were used as security ink. Based on the time-resolved characteristic, the true information, including the

"1895", the "JOB", the QR code, and the school badge, could be seen visibly attributed to the green phosphorescence emission (Figure 6C).

The time-dependent phosphorescence color (TDPC) materials play important roles in high-level information encryption and security. Recently, Lu and coworkers realized the TDPC property of CDs by binary salt matrices, namely inorganic NaCl and metal (Mg^{2+} or Ca^{2+} or Ba^{2+}) doping. In addition, the TDPC of the CDs could be excited by the UV irradiation at extent wavelengths. Based on these characteristics, these TDPC CDs were used for high-level information encryption. Firstly, only after the irradiation with 365 nm, the $CDs/Na_{0.5}Mg_{0.25}Cl$ exhibited the obvious TDPC property with the emission color turning from yellow to green. However, after removing the 254 and 430 nm irradiation, the phosphorescence color was green, without clearly visible changes. Furthermore, a 3D code with switchable phosphorescence colors was realized based on this material, which can realize a dynamic phosphorescence signal over time with a decryption wavelength of 365 nm (Figure 6D).

4. Conclusions and Perspective

Recently, both the AIEgens and RTP materials have exhibited attractive applications in the field of anti-counterfeiting and information encryption. Furthermore, AIEgens and RTP materials with stimulus-responsive property are essential to intelligent and high-level security designs, which can be applied to more application scenarios and elementary encryption and anti-counterfeiting technologies, for example ones based on time-resolved ability.

Undoubtedly, more and more stimuli-responsive AIEgens and RTP materials will be developed in the future, and it is worth looking forward to their important contributions in the information protection market. For further development of stimulus-responsive AIEgens and RTP materials, two types are highly expected: (a) the decryption of information depends on specific stimuli, such as a specific temperature or acidity; (b) combining with the functional matrix to obtain smart luminescent materials with multilevel responsive or multi-stimulus-responsive properties. In such cases, high levels of security and information protection could be realized.

Author Contributions: Conceptualization, Y.L. and P.G.; writing—original draft preparation, Y.L.; writing—review and editing, P.G.; supervision, P.G.; funding acquisition, P.G. All authors have read and agreed to the published version of the manuscript.

Institutional Review Board Statement: Not applicable.

Informed Consent Statement: Not applicable.

Data Availability Statement: Not applicable.

Conflicts of Interest: The authors declare no conflict of interest.

References

1. Li, L. Technology Designed to Combat Fakes in the Global Supply Chain. *Bus. Horiz.* **2013**, *56*, 167–177. [CrossRef]
2. Pyzik, O.Z.; Abubakar, I. Fighting the Fakes: Tackling Substandard and Falsified Medicines. *Nat. Rev. Dis. Primers* **2022**, *8*, 55. [CrossRef]
3. Quan, Z.; Zhang, Q.; Li, H.; Sun, S.; Xu, Y. Fluorescent Cellulose-Based Materials for Information Encryption and Anti-Counterfeiting. *Coordin. Chem. Rev.* **2023**, *493*, 215287. [CrossRef]
4. Li, H.; Zhu, M.; Tian, F.; Hua, W.; Guo, J.; Wang, C. Polychrome Photonic Crystal Stickers with Thermochromic Switchable Colors for Anti-Counterfeiting and Information Encryption. *Chem. Eng. J.* **2021**, *426*, 130683. [CrossRef]
5. Xu, F.-F.; Gong, Z.-L.; Zhong, Y.-W.; Yao, J.; Zhao, Y.S. Wavelength-Tunable Single-Mode Microlasers Based on Photoresponsive Pitch Modulation of Liquid Crystals for Information Encryption. *Research* **2020**, *2020*, 65394. [CrossRef]
6. Yang, T.; Wang, Y.; Duan, J.; Wei, S.; Tang, S.; Yuan, W.Z. Time-Dependent Afterglow from a Single Component Organic Luminogen. *Research* **2021**, *2021*, 9757460. [CrossRef]
7. Du, H.; Zhao, W.; Xia, Y.; Xie, S.; Tao, Y.; Gao, Y.Q.; Zhang, J.; Wan, X. Effect of Stereoregularity on Excitation-Dependent Fluorescence and Room-Temperature Phosphorescence of Poly(2-Vinylpyridine). *Aggregate* **2023**, *4*, e276. [CrossRef]

8. Wang, X.; Feng, J.; Yu, H.; Jin, Y.; Davidson, A.; Li, Z.; Yin, Y. Anisotropically Shaped Magnetic/Plasmonic Nanocomposites for Information Encryption and Magnetic-Field-Direction Sensing. *Research* **2018**, *2018*, 7527825. [CrossRef]

9. Guo, Q.; Zhang, M.; Tong, Z.; Zhao, S.; Zhou, Y.; Wang, Y.; Jin, S.; Zhang, J.; Yao, H.-B.; Zhu, M.; et al. Multimodal-Responsive Circularly Polarized Luminescence Security Materials. *J. Am. Chem. Soc.* **2023**, *145*, 4246–4253. [CrossRef]

10. Hu, Y.; Huang, Z.; Willner, I.; Ma, X. Multicolor Circularly Polarized Luminescence of a Single-Component System Revealing Multiple Information Encryption. *CCS Chem.* **2023**. [CrossRef]

11. Lin, S.; Tang, Y.; Kang, W.; Bisoyi, H.K.; Guo, J.; Li, Q. Photo-Triggered Full-Color Circularly Polarized Luminescence Based on Photonic Capsules for Multilevel Information Encryption. *Nat. Commun.* **2023**, *14*, 3005. [CrossRef]

12. Zhao, S.; Wang, Z.; Ma, Z.; Fan, F.; Liu, W. Achieving Multimodal Emission in $Zn_4B_6O_{13}$:Tb^{3+},Yb^{3+} for Information Encryption and Anti-Counterfeiting. *Inorg. Chem.* **2020**, *59*, 15681–15689. [CrossRef] [PubMed]

13. Gao, P.F.; Lei, G.; Huang, C.Z. Dark-Field Microscopy: Recent Advances in Accurate Analysis and Emerging Applications. *Anal. Chem.* **2021**, *93*, 4707–4726. [CrossRef] [PubMed]

14. Gao, P.F.; Zou, H.Y.; Gao, M.X.; Li, Y.F.; Huang, C.Z. Plasmonic Locator with Sub-Diffraction-Limited Resolution for Continuously Accurate Positioning. *Aggregate* **2022**, *3*, e167. [CrossRef]

15. Chen, X.; Jiang, Z.; Liang, L.; Li, Y.F.; Huang, C.Z.; Gao, P.F. Dark-Field Imaging Monitoring of Adenosine Triphosphate in Live Cells by Au NBPs@ZIF-8 Nanoprobes. *Anal. Chem.* **2022**, *94*, 18107–18113. [CrossRef]

16. Liu, J.J.; Wen, S.; Yan, H.H.; Cheng, R.; Zhu, F.; Gao, P.F.; Zou, H.Y.; Huang, C.Z.; Wang, J. The Accurate Imaging of Collective Gold Nanorods with a Polarization-Dependent Dark-Field Light Scattering Microscope. *Anal. Chem.* **2023**, *95*, 1169–1175. [CrossRef]

17. Xu, Y.; Li, Q.; He, W.; Yang, C.P.; Gao, P.F.; Li, Y.F.; Huang, C.Z. Visual Identification of $1O_2$-Induced Crystal Structure Transformation of Single Zr-MOF by Dark-Field Microscopy. *Chem. Commun.* **2023**, *59*, 5729–5732. [CrossRef] [PubMed]

18. Li, Q.; Xu, Y.; He, W.; Li, Y.F.; Gao, P.F.; Huang, C.Z. Plasmon-Dependent Photophysical Preparation of Reversible Au@Safranine T Core-Shell Nanostructures with Edit and Erase Features. *Appl. Surf. Sci.* **2023**, *619*, 156709. [CrossRef]

19. Yu, X.; Zhang, H.; Yu, J. Luminescence Anti-Counterfeiting: From Elementary to Advanced. *Aggregate* **2021**, *2*, 20–34. [CrossRef]

20. Liu, S.; Liu, X.; Yuan, J.; Bao, J. Multidimensional Information Encryption and Storage: When the Input Is Light. *Research* **2021**, *2021*, 7897849. [CrossRef]

21. Zhang, H.; Zhao, Z.; Turley, A.T.; Wang, L.; McGonigal, P.R.; Tu, Y.; Li, Y.; Wang, Z.; Kwok, R.T.K.; Lam, J.W.Y.; et al. Aggregate Science: From Structures to Properties. *Adv. Mater.* **2020**, *32*, 2001457. [CrossRef]

22. Tang, B.Z. Aggregology: Exploration and Innovation at Aggregate Level. *Aggregate* **2020**, *1*, 4–5. [CrossRef]

23. Hu, R.; Zhang, G.; Qin, A.; Tang, B.Z. Aggregation-Induced Emission (AIE): Emerging Technology Based on Aggregate Science. *Pure Appl. Chem.* **2021**, *93*, 1383–1402. [CrossRef]

24. Luo, J.; Xie, Z.; Lam, J.W.Y.; Cheng, L.; Chen, H.; Qiu, C.; Kwok, H.S.; Zhan, X.; Liu, Y.; Zhu, D.; et al. Aggregation-Induced Emission of 1-Methyl-1,2,3,4,5-Pentaphenylsilole. *Chem. Commun.* **2001**, *381*, 1740–1741. [CrossRef] [PubMed]

25. Mei, J.; Leung, N.L.C.; Kwok, R.T.K.; Lam, J.W.Y.; Tang, B.Z. Aggregation-Induced Emission: Together We Shine, United We Soar! *Chem. Rev.* **2015**, *115*, 11718–11940. [CrossRef] [PubMed]

26. Kang, M.; Zhang, Z.; Song, N.; Li, M.; Sun, P.; Chen, X.; Wang, D.; Tang, B.Z. Aggregation-Enhanced Theranostics: AIE Sparkles in Biomedical Field. *Aggregate* **2020**, *1*, 80–106. [CrossRef]

27. Duo, Y.; Luo, G.; Zhang, W.; Wang, R.; Xiao, G.G.; Li, Z.; Li, X.; Chen, M.; Yoon, J.; Tang, B.Z. Noncancerous Disease-Targeting AIEgens. *Chem. Soc. Rev.* **2023**, *52*, 1024–1067. [CrossRef] [PubMed]

28. Hu, J.-J.; Jiang, W.; Yuan, L.; Duan, C.; Yuan, Q.; Long, Z.; Lou, X.; Xia, F. Recent Advances in Stimuli-Responsive Theranostic Systems with Aggregation-Induced Emission Characteristics. *Aggregate* **2021**, *2*, 48–65. [CrossRef]

29. Li, Y.J.; Zhang, H.T.; Chen, X.Y.; Gao, P.F.; Hu, C.-H. A Multifunctional AIEgen with High Cell-Penetrating Ability for Intracellular Fluorescence Assays, Imaging and Drug Delivery. *Mater. Chem. Front.* **2019**, *3*, 1151–1158. [CrossRef]

30. He, X.; Xiong, L.-H.; Huang, Y.; Zhao, Z.; Wang, Z.; Lam, J.W.Y.; Kwok, R.T.K.; Tang, B.Z. AIE-Based Energy Transfer Systems for Biosensing, Imaging, and Therapeutics. *TrAC Trend. Anal. Chem.* **2020**, *122*, 115743. [CrossRef]

31. Niu, G.; Zhang, R.; Shi, X.; Park, H.; Xie, S.; Kwok, R.T.K.; Lam, J.W.Y.; Tang, B.Z. AIE Luminogens as Fluorescent Bioprobes. *TrAC Trend. Anal. Chem.* **2020**, *123*, 115769. [CrossRef]

32. Yang, J.; Fang, M.; Li, Z. Organic Luminescent Materials: The Concentration on Aggregates from Aggregation-Induced Emission. *Aggregate* **2020**, *1*, 6–18. [CrossRef]

33. Feng, X.; Xu, Z.; Hu, Z.; Qi, C.; Luo, D.; Zhao, X.; Mu, Z.; Redshaw, C.; Lam, J.W.Y.; Ma, D.; et al. Pyrene-Based Blue Emitters with Aggregation-Induced Emission Features for High-Performance Organic Light-Emitting Diodes. *J. Mater. Chem. C* **2019**, *7*, 2283–2290. [CrossRef]

34. Wang, M.; Liang, H.; Wang, L.; Zhang, H.; Wang, J.; Wei, Y.; He, X.; Yang, Y. First AIE Probe for Lithium-Metal Anodes. *Matter* **2022**, *5*, 3530–3540. [CrossRef]

35. Zhang, J.; He, B.; Hu, Y.; Alam, P.; Zhang, H.; Lam, J.W.Y.; Tang, B.Z. Stimuli-Responsive AIEgens. *Adv. Mater.* **2021**, *33*, 2008071. [CrossRef]

36. Xie, T.; Zhang, B.; Zhang, X.; Zhang, G. AIE-Active B-Diketones Containing Pyridiniums: Fluorogenic Binding to Cellulose and Water-Vapour-Recoverable Mechanochromic Luminescence. *Mater. Chem. Front.* **2017**, *1*, 693–696. [CrossRef]

37. Duan, C.; Zhou, Y.; Shan, G.-G.; Chen, Y.; Zhao, W.; Yuan, D.; Zeng, L.; Huang, X.; Niu, G. Bright Solid-State Red-Emissive Bodipys: Facile Synthesis and Their High-Contrast Mechanochromic Properties. *J. Mater. Chem. C* **2019**, *7*, 3471–3478. [CrossRef]

38. Zhang, J.; He, B.; Wu, W.; Alam, P.; Zhang, H.; Gong, J.; Song, F.; Wang, Z.; Sung, H.H.Y.; Williams, I.D.; et al. Molecular Motions in AIEgen Crystals: Turning on Photoluminescence by Force-Induced Filament Sliding. *J. Am. Chem. Soc.* **2020**, *142*, 14608–14618. [CrossRef]

39. Tu, Y.; Yu, Y.; Xiao, D.; Liu, J.; Zhao, Z.; Liu, Z.; Lam, J.W.Y.; Tang, B.Z. An Intelligent AIEgen with Nonmonotonic Multiresponses to Multistimuli. *Adv. Sci.* **2020**, *7*, 2003525. [CrossRef]

40. Zhang, J.; Li, A.; Zou, H.; Peng, J.; Guo, J.; Wu, W.; Zhang, H.; Zhang, J.; Gu, X.; Xu, W.; et al. A "Simple" Donor–Acceptor AIEgen with Multi-Stimuli Responsive Behavior. *Mater. Horiz.* **2020**, *7*, 135–142. [CrossRef]

41. Zheng, X.; Liu, X.; Liu, L.; Li, X.; Jiang, S.; Niu, C.; Xie, P.; Liu, G.; Cao, Z.; Ren, Y.; et al. Multi-Stimuli-Induced Mechanical Bending and Reversible Fluorescence Switching in a Single Organic Crystal. *Angew. Chem. Int. Ed.* **2022**, *61*, e202113073. [CrossRef]

42. Li, Z.; Liu, L.; Liu, Y. An AIE-Active Dual Fluorescent Switch with Negative Photochromism for Information Display and Encryption. *New J. Chem.* **2021**, *45*, 9872–9881. [CrossRef]

43. Liang, X.; Dong, B.; Wang, H.; Zhang, Z.; Wang, S.; Li, J.; Zhao, B.; Li, Z.; Xing, Y.; Guo, K. An AIE-Active Acridine Functionalized Spiro[Fluorene-9,9′-Xanthene] Luminophore with Mechanoresponsive Luminescence for Anti-Counterfeiting, Information Encryption and Blue Oleds. *J. Mater. Chem. C* **2022**, *10*, 7857–7865. [CrossRef]

44. Jiang, H.; Li, G.; Liu, F.; Guo, Y.; Wang, H.; Li, J.; Zhang, R.; Xia, Y.; Guo, K. Opposite Thermal-Stimuli Fluorescent Behavior Induced by π-Bridge in Two Carbazole Derivatives for High-Level Information Encryption. *Dyes Pigments* **2023**, *217*, 111437. [CrossRef]

45. Zuo, Y.; Liu, J.; Li, P.; Li, K.; Lam, J.W.Y.; Wu, D.; Tang, B.Z. Full-Color-Tunable AIE Luminogens for 4d Code, Security Patterns, and Multicolor Leds. *Cell Rep. Phys. Sci.* **2023**, *4*, 101202. [CrossRef]

46. He, X.; Zhang, J.; Liu, X.; Jin, Z.; Lam, J.W.Y.; Tang, B.Z. A Multiresponsive Functional AIEgen for Spatiotemporal Pattern Control and All-Round Information Encryption. *Angew. Chem. Int. Ed.* **2023**, *62*, e202300353. [CrossRef]

47. Zhang, J.; Shen, H.; Liu, X.; Yang, X.; Broman, S.L.; Wang, H.; Li, Q.; Lam, J.W.Y.; Zhang, H.; Cacciarini, M.; et al. A Dihydroazulene-Based Photofluorochromic AIE System for Rewritable 4d Information Encryption. *Angew. Chem. Int. Ed.* **2022**, *61*, e202208460. [CrossRef]

48. Yang, C.; Xiao, H.; Luo, Z.; Tang, L.; Dai, B.; Zhou, N.; Liang, E.; Wang, G.; Tang, J. A Light-Fueled Dissipative Aggregation-Induced Emission System for Time-Dependent Information Encryption. *Chem. Commun.* **2023**, *59*, 5910–5913. [CrossRef]

49. Deng, D.-d.; Zou, Y.; Chen, Z.; Liu, S.; Yang, Y.; Pu, S. Finely Regulated Benzothiadiazole Derivatives: Aggregation-Induced Emission (AIE), Hypso- or Bathochromic Mechanofluorochromic Behaviors, and Multilevel Information Encryption Applications. *Dyes Pigments* **2023**, *211*, 111051. [CrossRef]

50. Liu, Z.; Wang, W.; Liao, H.; Lin, R.; He, X.; Zheng, C.; Guo, C.; Liu, H.; Feng, H.-T.; Chen, M. Engineering Isomeric AIEgens Containing Tetraphenylpyrazine for Dual Memory Storage. *Chem. Biomed. Imaging* **2023**. [CrossRef]

51. Qin, M.; Xu, Y.; Gao, H.; Han, G.; Cao, R.; Guo, P.; Feng, W.; Chen, L. Tetraphenylethylene@Graphene Oxide with Switchable Fluorescence Triggered by Mixed Solvents for the Application of Repeated Information Encryption and Decryption. *ACS Appl. Mater. Interfaces* **2019**, *11*, 35255–35263. [CrossRef] [PubMed]

52. Sui, X.; Wang, X.; Cai, C.; Ma, J.; Yang, J.; Zhang, L. AIE-Active Freeze-Tolerant Hydrogels Enable Multistage Information Encryption and Decryption at Subzero Temperatures. *Engineering* **2023**, *23*, 82–89. [CrossRef]

53. Huang, J.; Liu, Y.; Lin, J.; Su, J.; Redshaw, C.; Feng, X.; Min, Y. Novel Pyrene-Based Aggregation-Induced Emission Luminogen (AIEgen) Composite Phase Change Fibers with Satisfactory Fluorescence Anti-Counterfeiting, Temperature Sensing, and High-Temperature Warning Functions for Solar-Thermal Energy Storage. *Adv. Compos. Hybrid Mater.* **2023**, *6*, 126. [CrossRef]

54. Yao, P.; Qiao, W.; Wang, Y.; Peng, H.; Xie, X.; Li, Z.A. Deep-Red Emissive Squaraine-AIEgen in Elastomer Enabling High Contrast and Fast Thermoresponse for Anti-Counterfeiting and Temperature Sensing. *Chem. Eur. J.* **2022**, *28*, e202200725. [CrossRef] [PubMed]

55. Wang, J.; Zhang, M.; Han, S.; Zhu, L.; Jia, X. Multiple-Stimuli-Responsive Multicolor Luminescent Self-Healing Hydrogel and Application in Information Encryption and Bioinspired Camouflage. *J. Mater. Chem. C* **2022**, *10*, 15565–15572. [CrossRef]

56. Yang, C.; Xiao, H.; Tang, L.; Luo, Z.; Luo, Y.; Zhou, N.; Liang, E.; Wang, G.; Tang, J. A 3D Multistage Information Encryption Platform with Self-Erasure Function Based on a Synergistically Shape-Deformable and AIE Fluorescence-Tunable Hydrogel. *Mater. Horiz.* **2023**, *10*, 2496–2505. [CrossRef]

57. Tao, Y.; Lin, J.; Wang, D.; Wang, Y. Na⁺-Functionalized Carbon Dots with Aggregation-Induced and Enhanced Cyan Emission. *J. Colloid Interf. Sci.* **2021**, *588*, 469–475. [CrossRef]

58. Yang, L.; Liu, S.; Quan, T.; Tao, Y.; Tian, M.; Wang, L.; Wang, J.; Wang, D.; Gao, D. Sulfuric-Acid-Mediated Synthesis Strategy for Multi-Colour Aggregation-Induced Emission Fluorescent Carbon Dots: Application in Anti-Counterfeiting, Information Encryption, and Rapid Cytoplasmic Imaging. *J. Colloid Interf. Sci.* **2022**, *612*, 650–663. [CrossRef]

59. Yang, H.; Liu, Y.; Guo, Z.; Lei, B.; Zhuang, J.; Zhang, X.; Liu, Z.; Hu, C. Hydrophobic Carbon Dots with Blue Dispersed Emission and Red Aggregation-Induced Emission. *Nat. Commun.* **2019**, *10*, 1789. [CrossRef]

60. Kou, X.; Li, L.; Mei, Q.; Dong, W.-F.; Wang, Y. Construction of Multi-Color Fluorescent Carbon Dots by Aggregation-Induced Emission. *Spectrochim. Acta A* **2022**, *279*, 121430. [CrossRef]

61. Zhang, G.; Palmer, G.M.; Dewhirst, M.W.; Fraser, C.L. A Dual-Emissive-Materials Design Concept Enables Tumour Hypoxia Imaging. *Nat. Mater.* **2009**, *8*, 747–751. [CrossRef] [PubMed]

62. Yuan, W.Z.; Shen, X.Y.; Zhao, H.; Lam, J.W.Y.; Tang, L.; Lu, P.; Wang, C.; Liu, Y.; Wang, Z.; Zheng, Q.; et al. Crystallization-Induced Phosphorescence of Pure Organic Luminogens at Room Temperature. *J. Phys. Chem. C* **2010**, *114*, 6090–6099. [CrossRef]
63. An, Z.; Zheng, C.; Tao, Y.; Chen, R.; Shi, H.; Chen, T.; Wang, Z.; Li, H.; Deng, R.; Liu, X.; et al. Stabilizing Triplet Excited States for Ultralong Organic Phosphorescence. *Nat. Mater.* **2015**, *14*, 685–690. [CrossRef] [PubMed]
64. Zhao, W.; He, Z.; Lam, J.W.Y.; Peng, Q.; Ma, H.; Shuai, Z.; Bai, G.; Hao, J.; Tang, B.Z. Rational Molecular Design for Achieving Persistent and Efficient Pure Organic Room-Temperature Phosphorescence. *Chemistry* **2016**, *1*, 592–602. [CrossRef]
65. Fateminia, S.M.A.; Mao, Z.; Xu, S.; Yang, Z.; Chi, Z.; Liu, B. Organic Nanocrystals with Bright Red Persistent Room-Temperature Phosphorescence for Biological Applications. *Angew. Chem. Int. Ed.* **2017**, *56*, 12160–12164. [CrossRef] [PubMed]
66. Fan, Y.; Liu, S.; Wu, M.; Xiao, L.; Fan, Y.; Han, M.; Chang, K.; Zhang, Y.; Zhen, X.; Li, Q.; et al. Mobile Phone Flashlight Excited Red Afterglow Bioimaging. *Adv. Mater.* **2022**, *34*, e2201280. [CrossRef]
67. Xiao, F.; Gao, H.; Lei, Y.; Dai, W.; Liu, M.; Zheng, X.; Cai, Z.; Huang, X.; Wu, H.; Ding, D. Guest-Host Doped Strategy for Constructing Ultralong-Lifetime near-Infrared Organic Phosphorescence Materials for Bioimaging. *Nat. Commun.* **2022**, *13*, 186. [CrossRef]
68. Huang, L.; Qian, C.; Ma, Z. Stimuli-Responsive Purely Organic Room-Temperature Phosphorescence Materials. *Chem. Eur. J.* **2020**, *26*, 11914–11930. [CrossRef]
69. Yang, J.; Fang, M.; Li, Z. Stimulus-Responsive Room Temperature Phosphorescence Materials: Internal Mechanism, Design Strategy, and Potential Application. *Acc. Mater. Res.* **2021**, *2*, 644–654. [CrossRef]
70. Cai, S.; Yao, X.; Ma, H.; Shi, H.; An, Z. Manipulating Intermolecular Interactions for Ultralong Organic Phosphorescence. *Aggregate* **2023**, *4*, e320. [CrossRef]
71. Ma, L.; Ma, X. Recent Advances in Room-Temperature Phosphorescent Materials by Manipulating Intermolecular Interactions. *Sci. China Chem.* **2023**, *66*, 304–314. [CrossRef]
72. Kabe, R.; Adachi, C. Organic Long Persistent Luminescence. *Nature* **2017**, *550*, 384–387. [CrossRef] [PubMed]
73. Zhang, X.; Du, L.; Zhao, W.; Zhao, Z.; Xiong, Y.; He, X.; Gao, P.F.; Alam, P.; Wang, C.; Li, Z.; et al. Ultralong UV/Mechano-Excited Room Temperature Phosphorescence from Purely Organic Cluster Excitons. *Nat. Commun.* **2019**, *10*, 5161. [CrossRef] [PubMed]
74. Chen, C.; Chi, Z.; Chong, K.C.; Batsanov, A.S.; Yang, Z.; Mao, Z.; Yang, Z.; Liu, B. Carbazole Isomers Induce Ultralong Organic Phosphorescence. *Nat. Mater.* **2021**, *20*, 175–180. [CrossRef] [PubMed]
75. Zhang, X.; Liu, J.; Chen, B.; He, X.; Li, X.; Wei, P.; Gao, P.F.; Zhang, G.; Lam, J.W.Y.; Tang, B.Z. Highly Efficient and Persistent Room Temperature Phosphorescence from Cluster Exciton Enables Ultrasensitive Off-on Voc Sensing. *Matter* **2022**, *5*, 3499–3512. [CrossRef]
76. Lei, Y.; Dai, W.; Guan, J.; Guo, S.; Ren, F.; Zhou, Y.; Shi, J.; Tong, B.; Cai, Z.; Zheng, J.; et al. Wide-Range Color-Tunable Organic Phosphorescence Materials for Printable and Writable Security Inks. *Angew. Chem. Int. Ed.* **2020**, *59*, 16054–16060. [CrossRef]
77. Chen, X.; Dai, W.; Wu, X.; Su, H.; Chao, C.; Lei, Y.; Shi, J.; Tong, B.; Cai, Z.; Dong, Y. Fluorene-Based Host-Guest Phosphorescence Materials for Information Encryption. *Chem. Eng. J.* **2021**, *426*, 131607. [CrossRef]
78. Dang, Q.; Jiang, Y.; Wang, J.; Wang, J.; Zhang, Q.; Zhang, M.; Luo, S.; Xie, Y.; Pu, K.; Li, Q.; et al. Room-Temperature Phosphorescence Resonance Energy Transfer for Construction of near-Infrared Afterglow Imaging Agents. *Adv. Mater.* **2020**, *32*, 2006752. [CrossRef]
79. Kuila, S.; George, S.J. Phosphorescence Energy Transfer: Ambient Afterglow Fluorescence from Water-Processable and Purely Organic Dyes Via Delayed Sensitization. *Angew. Chem. Int. Ed.* **2020**, *59*, 9393–9397. [CrossRef]
80. Li, G.; Jiang, D.; Shan, G.; Song, W.; Tong, J.; Kang, D.; Hou, B.; Mu, Y.; Shao, K.; Geng, Y.; et al. Organic Supramolecular Zippers with Ultralong Organic Phosphorescence by a Dexter Energy Transfer Mechanism. *Angew. Chem. Int. Ed.* **2022**, *61*, e202113425. [CrossRef]
81. Ma, L.; Xu, Q.; Sun, S.; Ding, B.; Huang, Z.; Ma, X.; Tian, H. A Universal Strategy for Tunable Persistent Luminescent Materials Via Radiative Energy Transfer. *Angew. Chem. Int. Ed.* **2022**, *61*, e202115748. [CrossRef] [PubMed]
82. Jinzheng, C.; Lin, F.; Liang, G.; Huang, H.; Tian, Q.; Yang, Z.; Chi, Z. Asymmetric Diarylamine Guests for Host-Guest System with Stimulus-Responsive Room Temperature Phosphorescence. *J. Mater. Chem. C* **2023**, *11*, 6290–6295.
83. Chanmungkalakul, S.; Wang, C.; Miao, R.; Chi, W.; Tan, D.; Qiao, Q.; Ang, E.C.X.; Tan, C.-H.; Fang, Y.; Xu, Z.; et al. A Descriptor for Accurate Predictions of Host Molecules Enabling Ultralong Room-Temperature Phosphorescence in Guest Emitters. *Angew. Chem. Int. Ed.* **2022**, *61*, e202200546. [CrossRef] [PubMed]
84. Wei, P.; Zhang, X.; Liu, J.; Shan, G.-G.; Zhang, H.; Qi, J.; Zhao, W.; Sung, H.H.Y.; Williams, I.D.; Lam, J.W.Y.; et al. New Wine in Old Bottles: Prolonging Room-Temperature Phosphorescence of Crown Ethers by Supramolecular Interactions. *Angew. Chem. Int. Ed.* **2020**, *59*, 9293–9298. [CrossRef] [PubMed]
85. She, P.; Lu, J.; Qin, Y.; Li, F.; Wei, J.; Ma, Y.; Wang, W.; Liu, S.; Huang, W.; Zhao, Q. Controllable Photoactivated Organic Persistent Room-Temperature Phosphorescence for Information Encryption and Visual Temperature Detection. *Cell Rep. Phys. Sci.* **2021**, *2*, 100505. [CrossRef]
86. Gao, W.; Liu, Z.; Dai, X.; Sun, W.; Gong, Q.; Li, J.; Ge, Y. Color-Tunable Ultralong Organic Phosphorescence: Commercially Available Triphenylmethylamine for Uv-Light Response and Anticounterfeiting. *Chem. Asian J.* **2023**, *18*, e202300450. [CrossRef]
87. Chen, H.; Yao, X.; Ma, X.; Tian, H. Amorphous, Efficient, Room-Temperature Phosphorescent Metal-Free Polymers and Their Applications as Encryption Ink. *Adv. Opt. Mater.* **2016**, *4*, 1397–1401. [CrossRef]

88. Su, Y.; Phua, S.Z.F.; Li, Y.; Zhou, X.; Jana, D.; Liu, G.; Lim Wei, Q.; Ong Wee, K.; Yang, C.; Zhao, Y. Ultralong Room Temperature Phosphorescence from Amorphous Organic Materials toward Confidential Information Encryption and Decryption. *Sci. Adv.* **2018**, *4*, eaas9732. [CrossRef]

89. Zhang, Y.; Wang, Z.; Su, Y.; Zheng, Y.; Tang, W.; Yang, C.; Tang, H.; Qu, L.; Li, Y.; Zhao, Y. Simple Vanilla Derivatives for Long-Lived Room-Temperature Polymer Phosphorescence as Invisible Security Inks. *Research* **2021**, *2021*, 8096263. [CrossRef]

90. Yang, Y.; Liang, Y.; Zheng, Y.; Li, J.-A.; Wu, S.; Zhang, H.; Huang, T.; Luo, S.; Liu, C.; Shi, G.; et al. Efficient and Color-Tunable Dual-Mode Afterglow from Large-Area and Flexible Polymer-Based Transparent Films for Anti-Counterfeiting and Information Encryption. *Angew. Chem. Int. Ed.* **2022**, *61*, e202201820. [CrossRef]

91. Liu, Y.; Xu, W.-W.; Chen, Y.; Qin, Y.-X.; Zhang, H.; Lu, Y.-L.; Xu, X. Tunable Second-Level Room-Temperature Phosphorescence of Solid Supramolecules between Acrylamide-Phenylpyridium Copolymers and Cucurbit[7]Uril. *Angew. Chem. Int. Ed.* **2022**, *61*, e202115265.

92. Zhao, J.; Yan, G.; Wang, W.; Shao, S.; Yuan, B.; Li, Y.J.; Zhang, X.; Huang, C.Z.; Gao, P.F. Molecular Thermal Motion Modulated Room-Temperature Phosphorescence for Multilevel Encryption. *Research* **2022**, *2022*, 9782713. [CrossRef] [PubMed]

93. Tian, Z.; Li, D.; Ushakova, E.V.; Maslov, V.G.; Zhou, D.; Jing, P.; Shen, D.; Qu, S.; Rogach, A.L. Multilevel Data Encryption Using Thermal-Treatment Controlled Room Temperature Phosphorescence of Carbon Dot/Polyvinylalcohol Composites. *Adv. Sci.* **2018**, *5*, 1800795. [CrossRef] [PubMed]

94. Cheng, M.; Cao, L.; Guo, H.; Dong, W.; Li, L. Green Synthesis of Phosphorescent Carbon Dots for Anticounterfeiting and Information Encryption. *Sensors* **2022**, *22*, 2944. [CrossRef] [PubMed]

95. Liu, F.; Li, Z.; Li, Y.; Feng, Y.; Feng, W. Room-Temperature Phosphorescent Fluorine-Nitrogen Co-Doped Carbon Dots: Information Encryption and Anti-Counterfeiting. *Carbon* **2021**, *181*, 9–15. [CrossRef]

96. Shi, W.; Wang, R.; Liu, J.; Peng, F.; Tian, R.; Lu, C. Time-Dependent Phosphorescence Color of Carbon Dots in Binary Salt Matrices through Activations by Structural Confinement and Defects for Dynamic Information Encryption. *Angew. Chem. Int. Ed.* **2023**, *62*, e202303063. [CrossRef]